01,09

Features of optical properties of semimetallic compounds ScBi and YBi

© Yu.V. Knyazev, Yu.I. Kuz'min

M.N. Mikheev Institute of Metal Physics, Ural Branch, Russian Academy of Sciences, Yekaterinburg, Russia

E-mail: knyazev@imp.uran.ru

Received June 26, 2023
Revised June 26, 2023
Accepted June 29, 2023

The results of experimental studies of the optical properties of binary cubic compounds ScBi and YBi are presented. The features of the frequency dispersion of dielectric functions in the wavelength range $0.22-15\,\mu$m are determined. The anomalous behavior of spectral characteristics in the infrared region of the spectrum corresponds to the semimetallic nature of these materials. A weak intraband contribution to low-energy optical conductivity is associated with the main feature of their electronic structure — the localization of the Fermi level in the region of a deep minimum of the density of states. The features of quantum light absorption are discussed on the basis of a comparative analysis of experimental and theoretical spectra of interband optical conductivity.

Keywords: semimetallic compounds, monopnictides, optical properties, electronic structure.

DOI: 10.61011/PSS.2023.09.57105.137

1. Introduction

Investigation of binary rare earth monopnictides RX (where R — Sc, Y, Ln, and X — V group p-elements) is of great interest due to versatile structural, electrical, magnetic and optical properties (see [1]), with some of them having good application prospects. Numerous such intermetallic compounds whose properties vary in a wide range, from metallic to semiconductor, have been synthesized recently. Potential applications of these materials are associated with demonstration of such properties as superconductivity, huge magnetoresistance, high magnetocaloric and magnetooptic effects [2–7]. The use of these intermetallic compounds as materials for optoelectronics is a promising area [8,9]. Doping of compounds with other elements as well as stoichiometry variation results in directional variation of numerous magnetic, electrical and thermodynamic parameters [10–12]. These monopnictides crystallize in a cubic lattice that at high pressures may be transformed into other types of structures [13,14]. Theoretical calculations have shown that a wide range of such intermetallic compounds have unusual electronic structure with irregularities typical for new quantum materials with unique physical properties — topological semimetals [15–18].

Such types of compounds include nonmagnetic binary intermetallic ScBi and YBi with NaCl-type cubic lattice that at 25 GPa and 23 GPa, respectively, is transformed into CsCl-type structure characterized by 5% decrease in volume [19]. Among the publications addressing experimental research of physical properties of rare earth monopnictides, there are just a few papers devoted to these compounds. It is shown, in particular, that these materials have low concentration of current carriers that is by two orders of magnitude lower than in good metals [20]. Moreover, the temperature dependence of resistance is of metallic type and grows steadily with temperature. The study of transport properties of intermetallic YBi has found extremely high magnetoresistance achieving 10^5% at low temperatures, and also metal−insulator transition induced by magnetic field [21,22].

Calculations of the electronic spectra of ScBi and YBi carried out recently within various calculation schemes have shown that there are several features in the structure and localization of Sc 3d-, Y 4d- and Bi 6p-states near the Fermi level E_F. The main of these features is the presence of a wide gap in the density of electronic states that results in semimetallic type of conductivity and predetermines high thermoelectric properties of these materials [19,23–28]. Hydrostatic pressure, as reported in the studies above, modifies the electronic spectra structure that, in turn, causes transformations of several physical properties, in particular, fast decrease of magnetoresistance and occurrence of superconductivity. Inversion of $d-p$ energy bands that takes place here results in significant change in dispersion of dielectric functions of these materials in a wide range of energies [25,28]. A unique property of the calculated band spectra of semimetallic ScBi and YBi is that topological features are predicted in them — gapless surface states, co-called Fermi arcs, defining significant difference in the charge transfer rates on the surface and in the volume. Recently, such properties useful for design of ultrafast electronic devices have been extensively studied theoretically and have been found experimentally in tantalum and niobium arsenides [29,30].

Additional information about the electronic structure of these compounds can be acquired from the investigation of spectral properties. For this, an optical ellipsometry method covering the wavelength range, including the UV, visible and IR regions, has been used herein. Experimental optical

conductivity spectra are compared with the spectra obtained from the previous ab initio band structure calculations.

2. Experiment

The studied polycrystalline ScBi and YBi samples were prepared by arc melting of stoichiometric proportions of high-purity metals (99.99%) in pure argon atmosphere. For homogenization, the prepared ingots were annealed in vacuum during a weak at $\sim 800^\circ$C. X-ray diffraction analysis of powder samples has shown that both alloys crystallize in the NaCl-type cubic structure with lattice parameters $a = 5.95$ Å (ScBi) and $a = 6.24$ Å (YBi) that is close to the values obtained previously in [23,24,31]. Flat mirror surfaces of the samples were prepared by successive polishing using diamond paste with different grain sizes.

Optical properties of the samples were studied by the ellipsometric method based on the measurement of amplitudes and phase shifts of the reflected light waves of s- and p-polarizations [32]. Within $\lambda = 0.22-15\,\mu$m (energies $E = 0.083-5.64$ eV), optical constants of the compounds were determined — refraction indices $n(\lambda)$ and absorption coefficients $k(\lambda)$. Measurements carried out at room temperature with accuracy 2–4%, cover the UV, visible and IR regions. $n(\lambda)$ and $k(\lambda)$ were used to calculate dispersion dependences of several functions characterizing the optical properties of the studied materials — real $\varepsilon_1 = n^2-k^2$ and imaginary $\varepsilon_2 = 2nk$ components of the complex permittivity, reflectivity $R = [(n-1)^2 + k^2]/[(n+1)^2 + k^2]$ and optical conductivity $\sigma = \varepsilon_2\omega/4\pi$ (ω — light frequency). Within the wavelength range, electromagnetic wave penetration depth $\delta = c/k\omega$ (c — speed of light) increases from several tens (UV region) to several hundreds of atomic layers (IR region) allowing to address the obtained optical parameters as bulk characteristics of the materials under study.

3. Results and discussion

Dependences of the optical constants of ScBi and YBi on the incident light wavelength are shown in Figure 1 (a short-wave range is shown in the detail). With increasing λ, significant growth of these parameters is observed. $k > n$ typical for metallic materials is satisfied throughout the wavelength range. Occurrence of peaks in the short-wave regions is associated with interband light absorption and steady dispersion above $\sim 1.5\,\mu$m is associated with intraband (Drude) light absorption. Energy dependences $\varepsilon_1(E)$, $\varepsilon_2(E)$ and $R(E)$ are shown in Figure 2. Behavior of these parameters with variation of the frequency of light is typical for conducting media. This becomes evident in the fact that $\varepsilon_1(E)$ remains negative at all energies, and an abrupt rise is observed on $\varepsilon_2(E)$ and $R(E)$ in the low-frequency range. It should be noted that relatively low $|\varepsilon_1|$ and R in the IR region are indicative of significant weaking

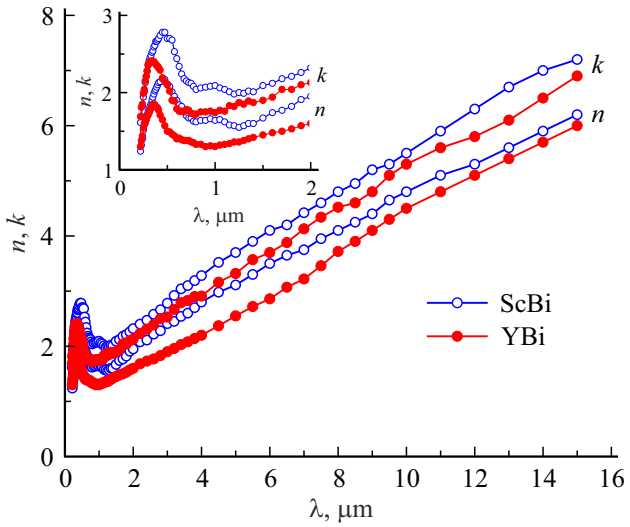

Figure 1. Dependence of the optical constants of ScBi and YBi on the incident light wavelength. A short-wave range is shown in the detail.

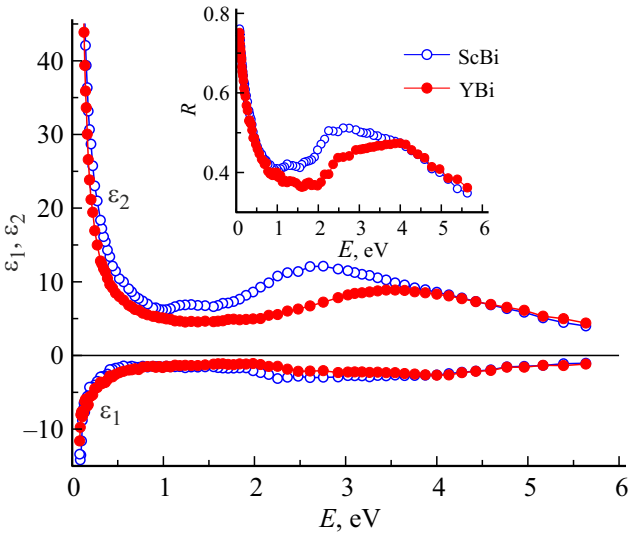

Figure 2. Real ε_1 and imaginary ε_2 components of permittivity and reflectivity R of ScBi and YBi.

of the metallic properties of these materials. Note that in good metals at $E < 0.1$ eV, $|\varepsilon_1|$ is by two to three orders of magnitude higher and the reflectivity R is close to unity [33].

The energy dependences of the optical conductivity of ScBi and YBi are shown in Figure 3 by circles. In the low-energy region, this parameter in both compounds is rather low and its growth can be seen only at the energies lower than ~ 0.2 eV. Such behavior of dispersion $\sigma(E)$ differs radically from the Drude dependence $\sigma \sim \omega^{-2}$ typical for metallic materials and exhibited in the IR frequency range. Similar abnormal behavior of this function was observed earlier for several compounds whose electronic structure features the presence of energy gap at the Fermi

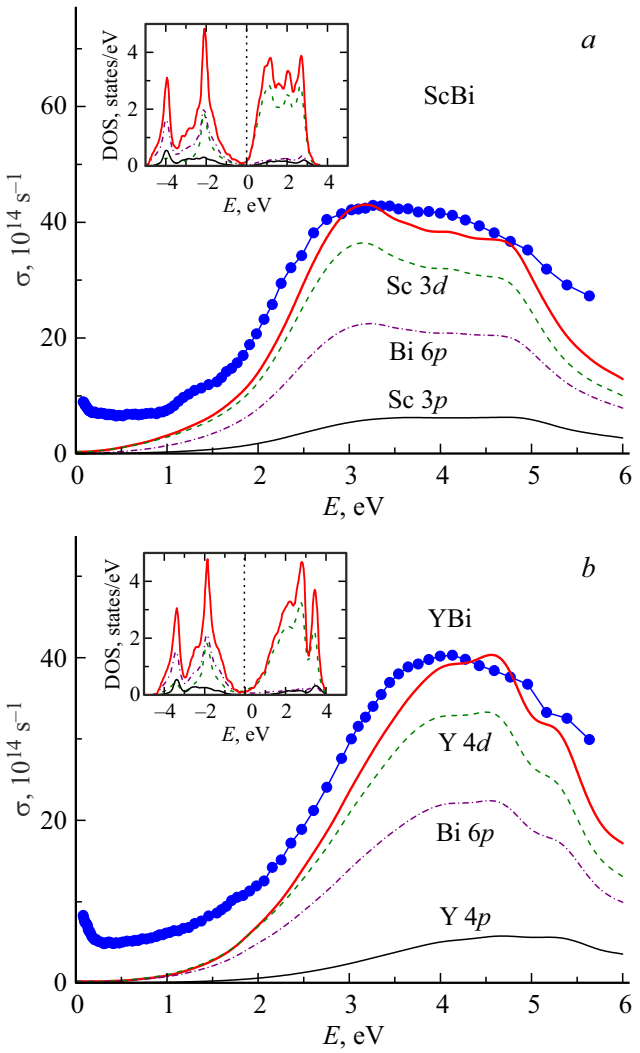

Figure 3. Experimental (circles) and calculated (thick solid line) energy dependences of optical conductivity of ScBi and YBi. Contributions of interband transitions with participation of Sc 3*d*, (Y 4*d*), Sc 3*p* (Y 4*p*) and Bi 6*p* states are also shown. The details show total and partial densities of states as specified in [19].

level [18,34,35]. With the increase of photon energy at $E \gtrsim 1$ eV, the optical conductivity grows, and interband absorption associated with quantum electron transitions from the occupied states to free ones is the prevailing mechanism of electronic excitation by light. Within the curves $\sigma(E)$ of both compounds, intense absorption bands with similar shapes and a peak in the UV band near 3.2 (ScBi) and 4.1 eV (YBi) are observed.

Features of the experimental optical conductivity dependences may be qualitatively explained using the calculations of band spectra and densities of electron states $N(E)$ described in [19] and generally corresponding results obtained in [23–26]. Calculations have shown that within $-5 < E_F < 5$ eV in $N(E)$ structure of intermetallic ScBi and YBi, Sc 3*d*, 3*p*-, Y 4*d*, 4*p*- and Bi 6*p*-bands prevail with their partial densities forming a set of intense peaks on both sides of E_F. *d*-bands have high densities both above and below the Fermi energy, while *p*-bands have high densities only at $E < E_F$. Partial contributions of *s*-states are moderate and distributed evenly over a wide energy region. These calculations [19] as shown in details in Figure 3 have defined the features of the $N(E)$ structure of the studied intermetallic compounds. The main of these features is the presence of a wide dip (pseudogap) near E_F, on the bottom of which the density of states achieves almost zero level. Such irregularity in the $N(E)$ spectrum causes low current carrier concentration in these materials and high electrical resistances [20–22] that are by an order of magnitude higher than that in good metals. Abnormally low $\sigma(E)$ in the low energy region and the absence of the Drude rise observed herein also suggest that the metallic properties of both compounds degrade allowing to consider the compounds as bad metals or semimetals.

Taking into account that the structure of the observed optical conductivity spectra is based on the real configuration of the electronic spectra of the compounds, it is interesting to compare the experimental $\sigma(E)$ with theoretical dependences derived from the published densities of states [19]. The interband optical conductivities have been calculated similar to the method previously used in [36] based on the convolutions of total $N(E)$ above and below E_F on the assumption of an equal probability of all types of transitions. Results of such calculations that are of qualitative type owing to the above mentioned approximation are shown in Figure 3 in arbitrary units. Theoretical optical conductivity curves show rather close agreement with the experimental dependences. Despite some distinctions in the structural elements, the calculated $\sigma(E)$ spectra adequately describe the observed picture of the interband optical absorption, localization and width of the main peaks. According to the electronic structure [19], the intense interband absorption in the studied compounds has similar behavior and is mainly associated with quantum transitions between the filled hybridized Sc 3*d* (Y 4*d*)- and Bi 6*p*-bands and free Sc 3*d* (Y 4*d*) states. Contribution of other electronic states is minor due to their low partial densities. Most significant contributions to the interband optical conductivity associated with various electronic states are shown in Figure 3.

Thus, strong interband light absorption at $\sim 2-6$ eV and the absence of the Drude contribution to the low energy spectrum region are the main features of the optical conductivity dispersion of ScBi and YBi. Such behavior of $\sigma(E)$ is directly associated with the peculiar structure of their densities of electronic states, i. e. with the presence of deep dips in the energy region adjacent to the Fermi level. Width of these features estimated from the experiment is at least 2 eV corresponding with the calculated values in [19,23–25]. In general, the observed frequency dispersion of the ScBi and YBi optical properties is indicative of the semimetallic properties of these materials.

4. Conclusion

Optical properties of the binary ScBi and YBi in $\lambda = 0.22-15\,\mu$m region have been studied experimentally. Optical constants $n(\lambda)$ and $k(\lambda)$ were measured by the ellipsometric method and used to determine the energy dependences of the dielectric functions, optical conductivities and reflectivities. Optical conductivity spectra structure in the intense interband light absorption region is satisfactory explained by the previously published ab initio calculations of the band structure of these intermetallic compounds. It has been shown that $\sigma(E)$ of the compounds in the low energy region is characterized by abnormally low values suggesting the presence of deep dips in their densities of electronic states near the Fermi level. The semimetallic type of conductivity of these materials predicted by the electronic structure calculations is confirmed by the optical investigations.

Funding

The study was carried out under the state assignment of the Ministry of Education and Science of the Russian Federation (topic „Electron“, No. 122021000039-4).

Conflict of interest

The authors declare that they have no conflict of interest.

References

[1] C.-G. Duan, R.F. Sabirianov, W.N. Mei, P.A. Dowben, S.S. Jaswal, E.Y. Tsymbal. J. Phys.: Condens. Matter **19**, 315220 (2007).
[2] L. Ye, T. Suzuki, C.R. Wicker, J.G. Checkelsky. Phys. Rev. B **97**, *8*, 081108(R) (2018).
[3] M.P. Volkov, N.N. Stepanov. Phys. Solid State **61**, *8*, 1416 (2019).
[4] E.J.R. Plaza, C.S. Alves, A.A. Coelho, S. Gama, P.J. von Ranke. J. Magn. Magn. Mater. **272–276**, 2373 (2004).
[5] W.J. Ban, D.S. Wu, B. Xu, J.L. Luo, H. Xiao. J. Phys.: Condens. Matter **31**, 405701 (2019).
[6] H. Gu, F. Tang, Y.-R. Ruan, J.-M. Zhang, R.-J. Tang, W. Zhao, R. Zhao, L. Zhang, Z.-D. Han, B. Qian, X.-F. Jiang, Y. Fang. Phys. Rev. Mater. **4**, *12*, 124204 (2020).
[7] M. Zhang, X. Wang, A. Rahman, R. Dai, Z. Wang, Z. Zhang. Phys. Rev. B **101**, *6*, 064106 (2020).
[8] E.M. Krivoy, A.P. Vasudev, S. Rahimi, R.A. Synowicki, K.M. McNicholas, D.J. Ironside, R. Salas, G. Kelp, D. Jung, H.P. Nair, G. Shvets, D. Akinwande, M.L. Lee, M.I. Brongersma. S.R. Bank. ACS Photonics **5**, 3051 (2018).
[9] F. Szmulowicz, K.G. Eyink. J. Nanophotonics **9**, *1*, 093078 (2015).
[10] M.E.A. Belhadj, H. Rached, D. Rached, S. Amari. Comput. Condens. Matter **16**, e00295 (2018).
[11] D.X. Li, Y. Haga, H. Shida, T. Suzuki. J. Appl. Phys. **80**, *1*, 264 (1996).
[12] D.X. Li, Y. Haga, H. Shida, T. Suzuki, T. Koide, G. Kido. Phys. Rev. B **53**, *13*, 8473 (1996).
[13] P. Pandit, V. Srivastava, M. Rajagopalan, S.P. Sanyal. Physica B: Condens. Matter **405**, *9*, 2245 (2010).
[14] R. Dubey, S. Singh, G. Kaur. Solid State Commun. **338**, 114465 (2021).
[15] Z. Li, D.-D. Xu, S.-Y. Ning, H. Su, T. Iitaka, T. Tohyama, J.-X. Zhang. Int. J. Mod. Phys. B **31**, *29*, 1750217 (2017).
[16] O. Pavlosiuk, M. Kleinert, P. Swatek, D. Kaczorowski, P. Wiśniewski. Sci. Rep. **7**, 12822 (2017).
[17] P. Wadhwa, T.J.D. Kumar, A. Shukla, R. Kumar. Solid State Commun. **358**, 114976 (2022).
[18] Yu.V. Knyazev, Yu.I. Kuz'min, S.T. Baidak, A.V. Lukoyanov. Solid State Sci. **136**, 107085 (2023).
[19] N. Acharya, S.P. Sanyal. Solid State Commun. **266**, 39 (2017).
[20] O. Pavlosiuk, P. Swatek, D. Kaczorowski, P. Wiśniewski. Phys. Rev. B **97**, *23*, 235132 (2018).
[21] C.Q. Xu, B. Li, M.R. van Delft, W.H. Jiao, W. Zhou, B. Qian, N.D. Zhigadlo, D. Qian, R. Sankar, N.E. Hussey, X. Xu. Phys. Rev. B **99**, *2*, 024110 (2019).
[22] B. Qian, F. Tang, Y.R. Ruan, Y. Fang, Z.D. Han, X.F. Jiang, J.-M. Zhang, S.Y. Chen, D.H. Wang. J. Mater. Chem. C **6**, *37*, 10020 (2018).
[23] M. Shoaib, G. Murtaza, R. Khenata, M. Farooq, R. Ali. Comput. Mater. Sci. **79**, 239 (2013).
[24] M. Kakihana, K. Nishimura, T. Takeuchi, Y. Haga, H. Harima, M. Hedo, T. Nakama, Y. Ōnuki. J. Phys. Soc. Jpn **88**, *4*, 044712 (2019).
[25] M. Narimani, S. Yalameha, Z. Nourbakhsh. Physica E **122**, 114199 (2020).
[26] S. Azzi, H. Boublenza, A. Zaoui, M. Ferhat. Comput. Mater. Sci. **65**, 331 (2012).
[27] A.K. Ahirwar, M. Aynyas, Y.S. Panwar, S.P. Sanyal. Adv. Mater. Res. **1141**, 39 (2016).
[28] M. Narimani, Z. Nourbakhsh. J. Phys. Chem. Solids **145**, 109537 (2020).
[29] B.Q. Lv, N. Xu, H.M. Weng, J.Z. Ma, P. Richard, X.C. Huang, L.X. Zhao, G.F. Chen, C.E. Matt, F. Bisti, V.N. Strocov, J. Mesot, Z. Fang, X. Dai, T. Qian, M. Shi, H. Ding. Nature Phys. **11**, 724 (2015).
[30] S.-Y. Xu, N. Alidoust, I. Belopolski, Z. Yuan, G. Bian, T.-R. Chang, H. Zheng, V.N. Strocov, D.S. Sanchez, G. Chang, C. Zhang, D. Mou, Y. Wu, L. Huang, C.-C. Lee, S.-M. Huang, B.K. Wang, A. Bansil, H.-T. Jeng, T. Neupert, A. Kaminski, H. Lin, S. Jia, M.Z. Hasan. Nature Phys. **11**, 748 (2015).
[31] M.N. Abdusalyamova, A.G. Chuiko, E.I. Shishkin, O.I. Rachmatov. J. Alloys Compd. **240**, *1–2*, 272 (1996).
[32] H. Fujiwara. Specroscopic Ellipsometry: Principles and Applications. John Wiley Sons, N.Y. (2007). 392 p.
[33] M.A. Ordal, L.L. Long, R.J. Bell, S.E. Bell, R.R. Bell, R.W. Alexander Jr., C.A. Ward. Appl. Opt. **22**, *7*, 1099 (1983).
[34] V. Bellani, G. Guizzetti, F. Marabelli, A. Piaggi, A. Borghesi, F. Nava, V.N. Antonov, Vl.N. Antonov, O. Jepsen, O.K. Andersen. Phys. Rev. B. **46**, *15*, 9380 (1992).
[35] W.R.L. Lambrecht. Phys. Rev. B **62**, *20*, 13538 (2000).
[36] Yu.V. Knyazev, A.V. Lukoyanov, Yu.I. Kuz'min, A.G. Kuchin, I.A. Nekrasov. Phys. Rev. B **73**, *9*, 094410 (2006).

Translated by E.Ilyinskaya